

# Superplastic behavior of coarse-grained Al–Mg–Zn alloys

Marco Antonio García-Bernal ·  
David Hernandez-Silva · Victor Sauce-Rangel

Received: 2 June 2005 / Accepted: 24 April 2006 / Published online: 31 January 2007  
© Springer Science+Business Media, LLC 2007

**Abstract** In the present study, the superplastic behavior of five Al–Mg–Zn alloys in coarse grain size condition has been studied. The alloys were melted, cast into ingots and hot rolled. The grain size of the rolled samples was 69, 45, 40, 30 and 35  $\mu\text{m}$ . Tensile test specimens were machined from the hot rolled plate in the rolling direction. Strain-rate-change (SCR) tests at temperatures between 300 and 450  $^{\circ}\text{C}$  and strain rates between  $1 \times 10^{-4}$  and  $1 \times 10^{-1} \text{ s}^{-1}$  were carried out to determine the strain rate sensitivity of the flow stress. Finally, elongation-to-failure tests were conducted at those temperatures and strain rates, where the alloys showed high strain rate sensitivity. A maximal elongation of 400% was obtained for the 3.89 wt.% Zn alloy. The results are explained in terms of solute drag creep as the principal deformation mechanism.

## Introduction

Superplasticity is the ability of a polycrystalline material to exhibit very high tensile elongation prior to failure. It is generally accepted that grain boundary sliding (GBS) accommodated by slip or diffusion is the main deformation mechanism for structural superplas-

ticity [1, 2]. Therefore, generally speaking, the most important microstructure requirement for superplasticity is a fine grain size that is stable at high temperatures. Often, the refinement of grain size is achieved by complicated thermomechanical processing, while microstructure stability at high temperatures is attained by second phase particles precipitated at grain boundaries. The microstructure stabilization at superplastic temperatures is not completely guaranteed by the presence of second phase particles due to the fact that, during superplastic deformation of fine-grained materials, grain growth is generally present. However, some alloys show superplastic properties even when they are not fine grained. Al–Mg base alloys are a good example of materials that do not need to be fine grained to show moderated superplastic elongation, making complex thermomechanical treatment unnecessary. This fact could be of interest for production of low cost aluminum alloys to be used in automobile industry for vehicle weight reduction. The study of high temperature ductility of aluminum–magnesium alloys in coarse-grained conditions could be interesting for other applications.

Superplasticity in the Al–Mg system has been reported in several references [3–7]. Watanabe et al. [3] showed that coarse-grained AA5083 (grain size of 39  $\mu\text{m}$ ) is not superplastic, showing elongations of only 160%, however, they found that copper addition of 0.6 wt.% make this alloy superplastic. Elongation of 700% at 550  $^{\circ}\text{C}$  at a strain rate of  $2.8 \times 10^{-3} \text{ s}^{-1}$  was measured. Grain size before superplastic deformation was less than 10  $\mu\text{m}$ . It was later demonstrated that moderated superplastic elongation could be achieved in the AA5083 aluminum alloy by reducing its grain size (<10  $\mu\text{m}$ ) through cold deformation and recrystallization.

---

M. A. García-Bernal · D. Hernandez-Silva (✉) ·  
V. Sauce-Rangel  
Department of Metallurgical Engineering, Instituto  
Politécnico Nacional-ESIQIE, Apdo. Postal 118-392, 07738  
Mexico, D.F., Mexico  
e-mail: dhs07670@yahoo.com

Elongations of 480–630% could be achieved at temperature of 550 °C and at strain rate between  $1 \times 10^{-5} \text{ s}^{-1}$  and  $1.2 \times 10^{-2} \text{ s}^{-1}$  [4–6]. Hsiao and Huang [7] obtained an elongation of 400% in the same alloy at a temperature of 250 °C and a strain rate of  $1 \times 10^{-3} \text{ s}^{-1}$ . (Sub)grain size was of 0.5  $\mu\text{m}$ .

Other experimental compositions have demonstrated that it is possible to obtain moderated superplastic elongations in coarse-grained Al–Mg alloys [8–12]. Woo et al. [8] investigate the superplastic behavior of Al–Mg alloys with magnesium contents of 5.3, 7 and 11 wt.% Mg. The Alloy with 7 wt.% Mg exhibited the best ductility of 350% at 450 °C and strain rate  $1 \times 10^{-2} \text{ s}^{-1}$ . This alloy had a grain size of 130  $\mu\text{m}$ . Hosokawa et al. [9] studied the effect of silicon on deformation behavior of coarse-grained Al–4.5Mg alloys and showed elongations above 350% in this alloys in coarse grain size condition (grain size of 53  $\mu\text{m}$ ).

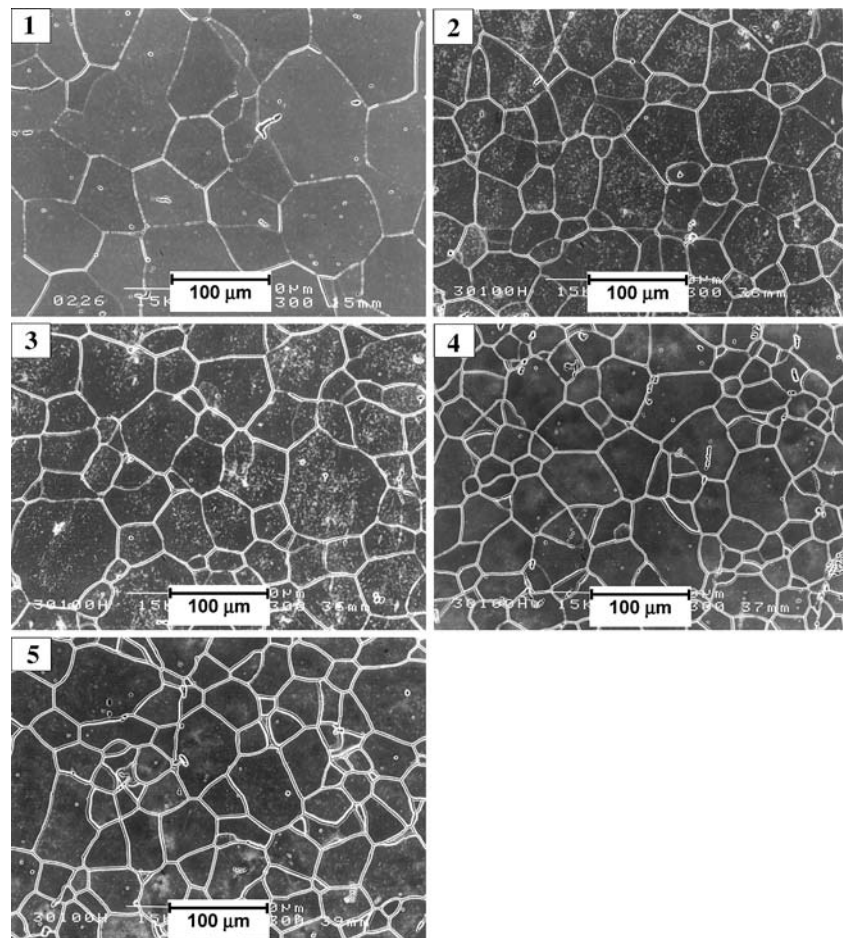
Coarse grain size Al–Mg alloys are believed to deform by a solute-drag-creep mechanism [11, 12]. In this mechanism, the creep rate is controlled by the

velocity of solute drag along with the dislocation line and is proportional to the third power of stress in contrast to the approximately two power of stress dependence observed in superplastic materials. In this system the high solubility of magnesium in aluminum at high temperature plays an important role. It could be reasonable to assume that other elements that form solid solutions with aluminum could show the same drag effect as with magnesium. Zinc is the element that has the greatest solubility in aluminum and the atomic size difference with aluminum is smaller than with magnesium, so it could possible that zinc atoms could have an effect on this creep mechanism and on the ductility of these alloys. It is the goal of this work to investigate the combined effect of magnesium and zinc in the ductility of these ternary alloys.

### Experimental procedure

Five Al–Mg–Zn were prepared using aluminum (purity 99.7%), magnesium (purity 99.9%) and zinc (purity

**Fig. 1** SEM-micrographs of the five alloys obtained after rolling at 380 °C. Grain sizes were 69, 45, 40, 30 and 35  $\mu\text{m}$  for alloy 1, 2, 3, 4 and 5, respectively



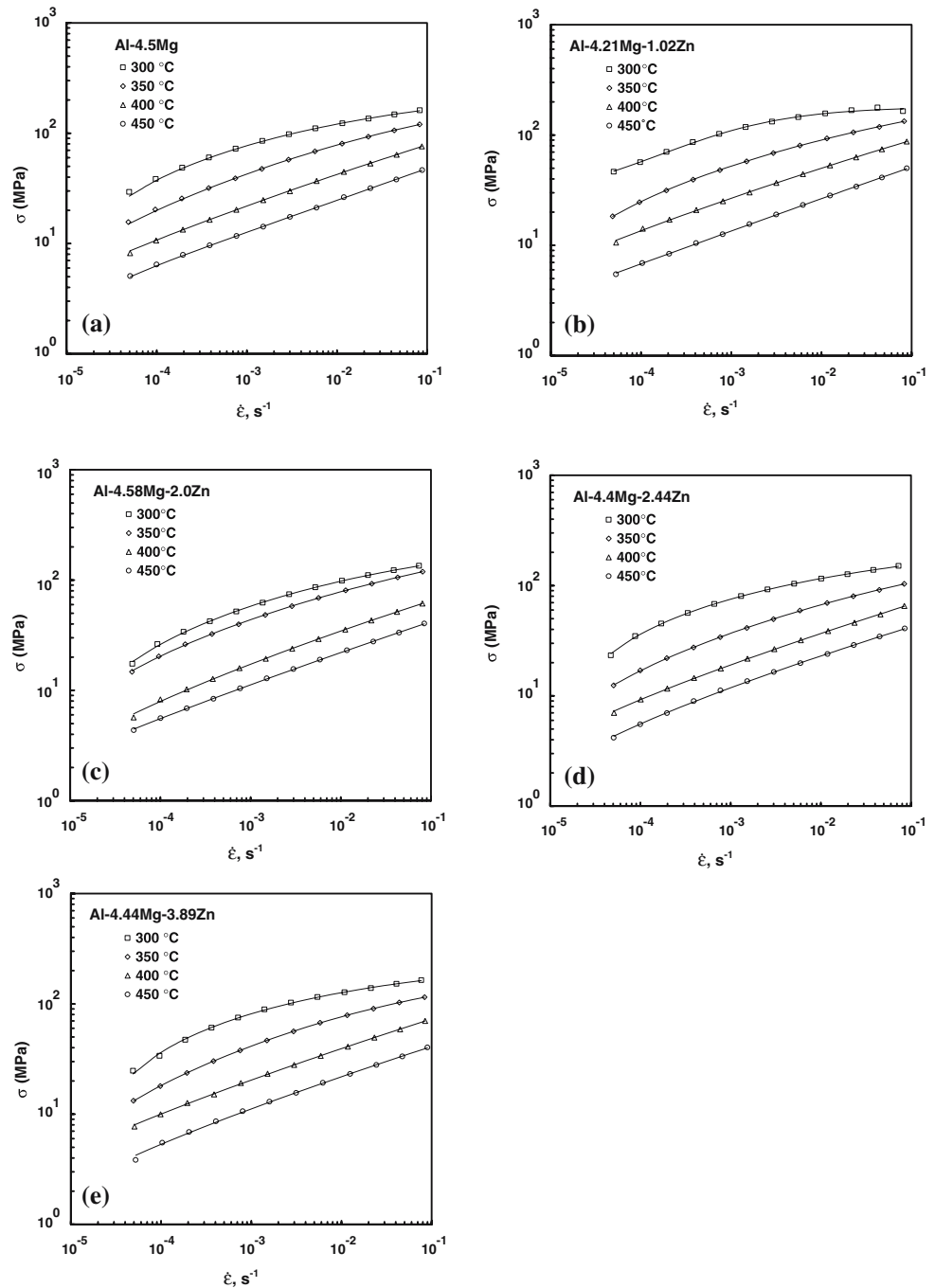
99.9%). Chemical composition, as obtained by wet chemistry, is shown in Table 1.

The alloys were melted in an electrical furnace in argon atmosphere in a graphite crucible and cast into a preheated steel mold. Argon gas was used as degassing agent. The ingots with dimensions of  $25 \times 80 \times 100$  mm were given an homogenization heat treatment at  $430^\circ\text{C}$  for 72 h and then hot-rolled at  $380^\circ\text{C}$  in several passes

**Table 1** Compositions in wt.% of the five alloys (remainder Al)

Alloy	Mg	Zn	Fe	Si
1	4.50	0.00	0.05	0.04
2	4.21	1.02	0.05	0.04
3	4.58	2.00	0.05	0.04
4	4.40	2.44	0.06	0.04
5	4.44	3.89	0.05	0.04

**Fig. 2** Temperature dependence of true stress versus true strain rate, (a) alloy 1, (b) alloy 2, (c) alloy 3, (d) alloy 4 and (e) alloy 5



(10% reduction per pass) to a final thickness of 5 mm. Tensile test specimens (5 mm gage width, 3.5 mm gage thickness and 15 mm gage length) were machined from the rolled plate with the tensile axes parallel to the rolling direction. Strain-rate-change (SCR) tests and elongation-to-failure tests were performed on a screw-driven testing machine. For SCR tests, an initial strain of 15% was imposed at a slow strain rate in order to set the grips and allow for microstructure stabilization to occur.

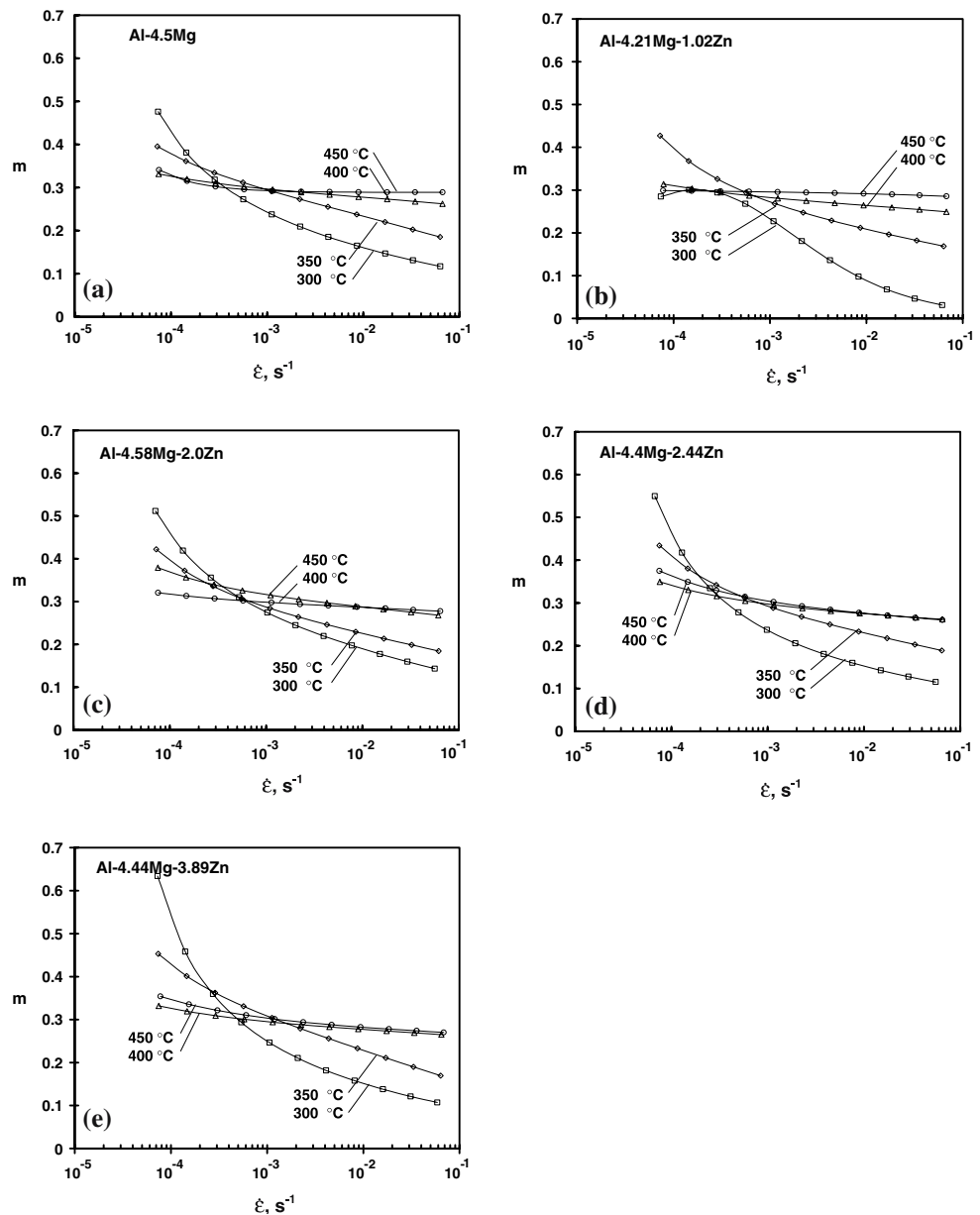
Strain-rate-change tests were carried out at 300, 350, 400 and 450 °C to determine the strain rate sensitivity of the flow stress, which is described by the expression  $\sigma = K \dot{\epsilon}^m$ . In this expression  $\dot{\epsilon}$  is the true strain rate,  $m$  is the strain rate sensitivity exponent,  $K$  is a constant and  $\sigma$  is the true stress. The specimens were pulled at

strain rates between  $10^{-4}$  and  $10^{-1} \text{ s}^{-1}$ . Elongation-to-failure tests were performed under a constant cross-head speed condition at those temperatures and strain rates, where the alloys showed high  $m$ -values. Specimens after rolling and after elongation-to-failure tests were etched with 0.1 vol.% HF and examined by means of scanning electron microscopy. Grain size was measured by the linear intercept method.

**Results and discussion**

In order to properly reveal the microstructure, the as-rolled samples were solution heat treated at 450 °C for 15 min and then water quenched followed by an aging

**Fig. 3** Flow stress and strain rate sensitivity index  $m$  as a function of strain rate at four different temperatures for all five alloys



treatment at 150 °C for 72 h. The microstructures of the five alloys are shown in Fig. 1. They consist of recrystallized grains with a precipitated phase of  $\text{Al}_3\text{Mg}_2$  containing Zn along the grain boundaries. The grain size of the alloys was 69, 45, 40, 30, and 35  $\mu\text{m}$  for alloys 1, 2, 3, 4 and 5, respectively.

Figure 2 shows the dependence of flow stress on strain rate, plotted on a double logarithmic scale at several temperatures. All alloys show approximately the same strength level especially at temperatures higher than 350 °C, however, as the temperature increases the level of stress decreases and the curve shape changes from curve toward a flatter configuration. The slope of these curves represents the strain rate sensitivity parameter  $m$ .

The  $m$  exponent for all alloys is shown in Fig. 3. At temperatures of 300 and 350 °C the  $m$  exponent is high (0.4–0.6) at low strain rates but decreases rapidly at high strain rates. On the other hand, at temperatures of 400 and 450 °C the  $m$  exponent is low (0.3–0.4) at low strain rates and decreases very slowly at high strain rates showing values of 0.3 at strain rates as high as  $8 \times 10^{-2} \text{ s}^{-1}$ .

Values of the exponent  $m$  in excess of 0.5 were observed at strain rates of  $1 \times 10^{-4} \text{ s}^{-1}$ . The fact that

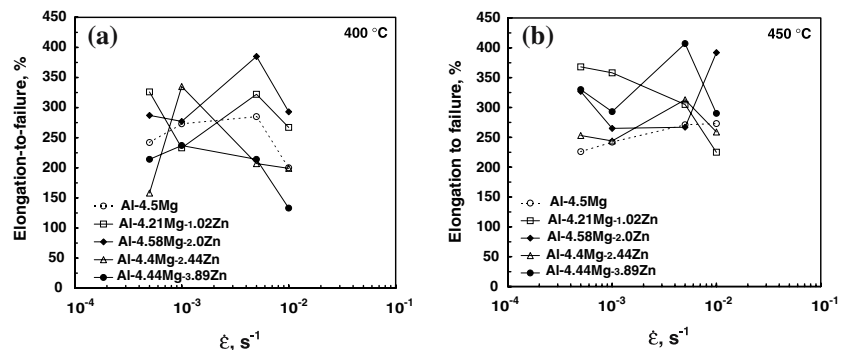
these values could be observed in coarse grain size alloys suggest that other deformation mechanism (e.g. grain boundary sliding) could play an important role at such low strain rates.

Figure 4 shows the elongation-to-failure as a function of the strain rate and zinc content at temperatures of 400 and 450 °C. The results show wide dispersion and do not show a clear effect of the zinc content on the maximal elongation. However, a maximal elongation of 400% was achieved in alloy with 2.0 wt.% Zn at 400 °C at a strain rate of  $5 \times 10^{-3} \text{ s}^{-1}$ . An elongation of 407% was achieved in alloy with 3.89 wt.% zinc at 450 °C and a strain rate of  $5 \times 10^{-3} \text{ s}^{-1}$ . At a high strain rate of  $10^{-2} \text{ s}^{-1}$  an elongation of 380% was achieved in alloy with 2.0 wt.% Zn at 450 °C.

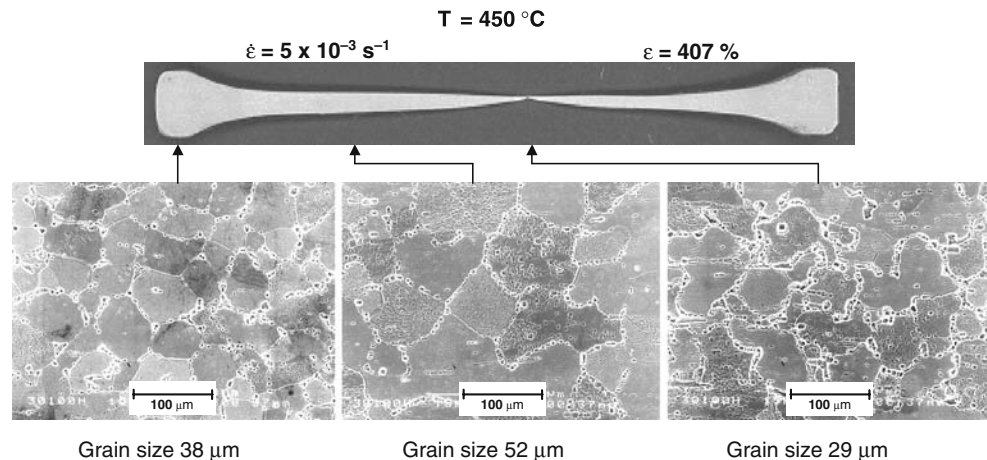
On the same figure are plotted in dashed line elongations obtained for alloy Al–4.5Mg. It was observed that especially at 450 °C the zinc addition had a positive effect on elongations, being in some cases around 100% higher than for alloy Al–4.5Mg.

Figure 5 shows micrographs of three different points of a superplastically deformed sample. The inter-mediate region between grip and fracture show a larger grain size compared to the grip and fracture regions. Superplastic materials generally show grain growth

**Fig. 4** Elongation-to-failure as a function of strain rate at (a) 400 and (b) 450 °C for the five alloys



**Fig. 5** SEM-micrographs of the alloy 5 after deformation at 450 °C and  $5 \times 10^{-3} \text{ s}^{-1}$ , illustrating the microstructures of three different regions



during high temperature deformation. This growth depends generally on strain. It could be to expect that the region near fracture would show coarser grain size than the rest of the sample, since this region suffered the largest strain. This result suggests that dynamic recrystallization could have taken place during deformation. This could explain the grain size refinement in the fracture region.

The elongation observed in these coarse-grained alloys can not be explained in terms of grain boundary sliding, the main deformation mechanism of fine grained superplastic materials. A mechanism in terms of dislocation-controlled creep seems to be the best explanation in this case. In this mechanism an exponent  $m = 0.33$  is expected as well as a creep rate that is independent on grain size. These two facts are consistent with the results found in this work.

Cavitation of the sample in Fig. 5 near fracture surface was evaluated using image analysis and was found to be less than 1 vol.%, which can be considered low.

Figure 6 shows true stress as a function of true strain rate for alloy 3.89 wt.% Zn. It can be seen a sharp peak stress after reaching the yield point, which is characteristic of viscous dislocation glide creep [9]. No strain hardening was observed.

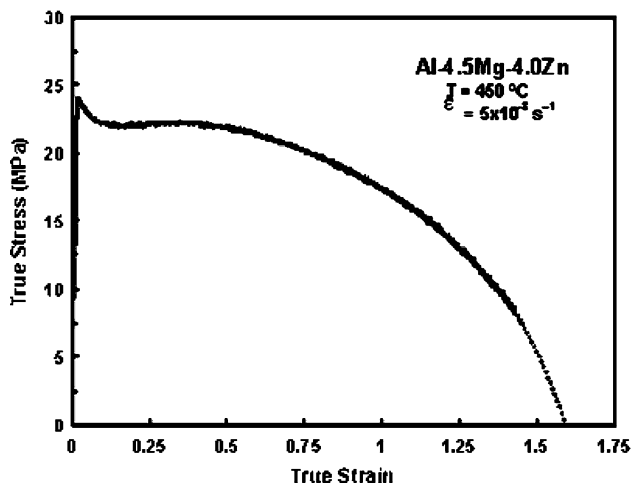


**Fig. 6** True stress as a function of true strain rate for alloy 3.88 wt.% Zn. No strain hardening was observed and a sharp decrease in flow stress after reaching the yield point was observed

## Conclusions

1. High tensile elongations were observed in the Al–Mg–Zn alloys studied. Maximal elongation of 407% was observed for alloy 3.89 wt.% Zn at 450 °C at a strain rate of  $5 \times 10^{-3} \text{ s}^{-1}$ .
2. It was observed that, in general, zinc addition has a positive effect on ductility when compared with alloys of similar magnesium content without zinc at the same test conditions.
3. Contrary to the grain growth generally observed on materials that deform by a grain boundary sliding mechanism, moderated grain refinement was observed during deformation of the deformed alloys in coarse-grained condition. Grain size of 38  $\mu\text{m}$  was refined to approximately 29  $\mu\text{m}$  near fracture region after a deformation of 400% for alloy with 3.89 wt.% Zn. This refinement was explained in terms of dynamic recrystallization as a consequence of dislocation-controlled creep deformation.

**Acknowledgements** This work has been supported by Instituto Politécnico Nacional and CONACYT (México). One of the authors (DHS) is recipient of COFAA-IPN and SNI fellowship.

## References

1. Sherby OD, Wadsworth J (1989) Prog Mater Sci 33:166
2. Edington JW, Melton KN, Cutler CP (1976) Prog Mater Sci 21(2):61
3. Watanabe H, Ohori K, Takeuchi Y (1987) Trans Iron Steel Inst Japan 27:730
4. Verma R, Ghosh AK, Kim S, Kim C (1995) Mater Sci Eng A191:143
5. Friedman PA, Ghosh AK (1996) Metall Mater Trans 27A:3027
6. Verma R, Friedman PA, Ghosh AK, Kim S, Kim C (1996) Metall Mater Trans 27A:1889
7. Hsiao IC, Huang JC (1999) Scripta Mater 40(6):697
8. Woo SS, Kim YR, Shin DH, Kim WJ (1997) Scripta Mater 37(9):1351
9. Hosokawa H, Iwasaki H, Mori T, Mabuchi M, Tagata T, Higashi K (1999) Acta Mater 47(6):1859
10. Sun IG Hong (1999) Scripta Mater 40(2):217
11. Kannan K, Johnson CH, Hamilton CH (1988) Metall Mater Trans A 29A:1211
12. Taleff EM, Henshall GA, Nieh TG, Lesuer DR, Wadsworth J (1998) Metall Mater Trans 29A:1081